B1313

Accelerated calendar life testing for SOFC: Impact of overpotential

Alexandra Ploner (1), Anke Hagen (1), Anne Hauch (1), Rémi Costa (2), Matthias Riegraf (2), Günter Schiller (2)
(1) Technical University of Denmark, Department of Energy Conversion and Storage
Frederiksborgvej 399, DK-4000 Roskilde/Denmark
(2) German Aerospace Center (DLR), Institute of Engineering Thermodynamics
Pfaffenwaldring 38-40, D-70569 Stuttgart/Germany
Tel.: +45-93511509
aplo@dtu.dk

Abstract

Substantial research activities in the last decades were dedicated to improve the durability of Solid Oxide Fuel Cells (SOFCs) to reach commercial viability targets. However, a lifetime of 40.000 – 80.000 h is needed to be economically competitive with current technologies and the estimation of lifetime as well as reliability of cells still remain critical issues [1].

Accelerated tests (AT) are a valuable approach to derive reliability and lifetime information and are routinely applied for various technologies, e.g. batteries and microelectronics [2]. Different methodologies are employed in this area, i.e. qualitative ATs to assess device reliability, and quantitative ATs which perform testing at a specific accelerating parameter and utilize models to allow extrapolation to the nominal operating level [3]. Yet, so far this method is not commonly used in the field of SOFC.

Many experimental results show that in the state-of-the-art SOFC technology, microstructural changes of the fuel electrode (Ni coarsening, loss of Ni-Ni contact) and Cr-poisoning of the oxygen electrode seem to be the core degradation phenomena [4,5]. While the fuel electrode was shown to dominate the initial degradation, the contribution of the cathode progressively takes over. The initial degradation rate often seen in SOFC voltage degradation tests causes challenges in reporting degradation rates and forces long-term measurements due to the underlying coarsening phenomenon [6]. Therefore, it is certainly beneficial to focus on accelerating the initial degradation trend to significantly shorten needed testing times.

Various previous studies - not only on Ni-YSZ electrodes but also on Ni-supported catalysts - suggest the use of steam partial pressure in the fuel and temperature as possible acceleration variables [7]. However, as SOFC can be operated in either galvano- or potentiostatic mode, current density or overpotential are additional relevant parameters in the context of ATs. This study is dedicated to evaluate the impact of fuel electrode overpotential on fuel electrode degradation via comparison of four 1000 h tests and proposes a methodology to assess this specific parameter for durability tests and lifetime prediction.

Introduction

Prediction of lifetime and degradation of Solid Oxide Fuel Cells (SOFCs) is a key challenge for successful market introduction. In case of stationary application, the lifetime of SOFCs should exceed at least five years to become an economically feasible option. Assessing lifetime of devices is generally a delicate challenge, since in many cases testing over the whole lifespan is pricy and tests cannot meet the needed technological progress. Therefore, lifetime and quality estimations based on accelerated testing (AT) methodologies are used to shorten the normal time of the degradation process [3,8,9]. Lifetime of a device is normally associated with its reliability and durability. These concepts are tested via two complementary but different methodologies, i.e. qualitative and quantitative AT. Whereas the first method is motivated to increase the break-down strength of a device (reliability), the second method is designated to understand the kinetics of degradation phenomena upon normal use and under elevated '*stress*' conditions (durability). In this context the term *'stress'* should not be mistaken with the more common meaning of mechanical stress but refers to conventional SOFC operating conditions, e.g. i.e. current density, temperature, etc.

The second approach in turn may be separated into '*calendar life'* (testing under constant testing conditions) or '*cycle life'* (periodically varying testing conditions) for SOFC testing, similarly to quantitative lifetime prediction of other electrochemical cell technologies. Previous performed '*calendar life'* SOFC tests targeted the influence of operating conditions such as temperature [10,11], current density [10], fuel/oxidant flow rate [12] or steam partial pressure [13,12]. '*Cycle life'* testing focused on evaluating degradation under ordinary shut-down and start-up conditions (temperature cycles) or due to power demand variations (current cycles) [14,15,16]. In these cases, the cycle frequency may be additionally considered as '*stress*' variable.

In most cases, lifetime prediction based on physical-chemical theory is a tedious and complex challenge if aging of a device consists of a variety of degradation mechanisms. In the experimentally based AT approach the influence of a *'stress'* is commonly predicted by semi-empirical models. Primarily, it is crucial to identify the critical degradation phenomena and to understand the impact of operating conditions and time. For SOFCs, the initial degradation period is often governed by microstructural changes of the fuel electrode [17] and due to the time-dependent nature of the process, it complicates lifetime prediction for durability tests which are given insufficient time. Based on common experience dominating sintering processes can span from a few 100 h up to 1.5 months (ca. 1000 h) [12]. To shorten testing times, it is therefore favorable to focus on this precise phenomenon to minimize test duration. Therefore, this study aims for an experimentally based *'calendar life'* AT approach concerning Ni-YSZ based electrodes and proposes a semi-empirical model for degradation prediction.

Furthermore, reliable metrics for degradation and end-of-life (EoL) need to be defined to allow lifetime prediction. Degradation is often reported by electrochemical terms, i.e. area specific resistance (ASR) or voltage loss in % based on the initial value. However, various researchers have addressed the pitfalls of these metrics as degradation rate (DR) and thus EoL depends on the operating parameters [18,19,20,21]. Appropriate comparison for degradation may currently only be possible via standardized testing conditions. Such activities have been pursued for SOFC since 2010 in different projects.

However, another valuable option would be to parametrize degradation on material specific properties. This methodology does not rely on standardized testing conditions, as

it the degradation metric is a material specific property. The present study is considering this possibility by proposing material specific degradation metrics for Ni-YSZ based fuel electrode and correlates it with a standardized electrochemical degradation metric.

Experimental

Reduction and cell testing

The electrochemical tests on four single cells were carried out in galvanostatic mode in a single furnace equipped with four separate cell test positions to guarantee most reproducible results. All single cells were planar, fuel electrode supported Ni-YSZ based SOFCs with an active area of 4 cm x 4 cm. In detail, the cells consists of an approx. 300 µm thick porous Ni-3YSZ support on a 12-15 µm Ni-8YSZ electrode, a ca.10 µm YSZ electrolyte and a 30 µm thick LSCF-CGO based oxygen electrode applied via screen printing on a 5 µm thick CGO barrier layer. The testing procedure started by heating the single cells to 850°C. Reduction of NiO in support and fuel electrode was initiated by supplying a flow of 5:95 H_2:Ar gas mixture at 20 l h^{-1} for 2 h and was completed for 1 h in pure H_2 at 20 l h^{-1}. Prior to long-term testing, the cells were characterized by iV-curves and Electrochemical Impedance Spectroscopy (EIS) at open circuit voltage (OCV) and different gas compositions on fuel and oxygen electrode. The characterizations were performed at T=850°C and T=750°C respectively. After testing the cells, a final characterization was performed and the cells were cooled down to room temperature in dry forming gas.

The test was split into two parts and testing conditions are summarized in Table 1.The first part (part A) of the test was conducted in high steam containing fuel. The investigated 'stress variable' in part B for cells 1-3 was the current density applied for galvanostatic testing while maintaining FU. This could be achieved by distributing the overall fuel supply of the testing station via adjustment of four separate mass-flow controllers towards each of the four testing positions and thus supplying fuel according to the chosen operating current density. Additionally a correction factor for fuel by-pass at each testing position was evaluated before test part B started. The correction factor was determined by performing iV-curves with visible mass-transfer limitations for each testing position and via comparison of the experimentally determined FU and the theoretical FU value a correction factor for the individual testing position was obtained.

The fourth cell (cell 2b) was operated at 0.75 A cm^{-2} with a different FU of approx. 40%. These conditions were chosen to operate cell 2b at a similar initial charge-transfer overpotential of the Ni-YSZ electrode as cell 2a but different mass-transfer overpotential.

Table 1 Testing specification of cell testing part A and B

	cell	$p(H_2O)_{in}$	time / h	T / °C	j / A cm^{-2}	FU / %
PART A	1	0.7	350	750	1	18*
	2a	0.7	350	750	1	18*
	3	0.7	350	750	0.5	9*
	2b	0.7	350	750	0.5	9*
PART B	1	0	1000	750	0.5	ca. 70
	2a	0	1000	750	0.687	ca. 70
	3	0	1000	750	1.25	ca. 70
	2b	0	1000	750	0.75	ca. 40

*given is the theoretical value, correction factor was not determined for these flow settings

Impedance Modeling

The initial cell characterization at different gasses and temperature conditions was used for qualitative impedance analysis and allowed assigning different electrochemical responses to the individual components, i.e. fuel electrode, oxygen electrode and electrolyte. Quantitative evaluation of the correlated ASR values is based on work by *Ramos et al.* [22].

Overpotential Quantification

Determination of the fuel electrode overpotential was done via EIS measurements at three to four different current density steps in the linear regime of the iV-curve before part B of the galvanostatic cell test (see Figure 1). The current steps measurements were conducted at the same temperature and gas composition conditions as part B of the test.

Quantitative analysis of the EIS via equivalent circuit modelling at each current density step allowed obtaining separate ASR contributions affecting fuel electrode resistance. The individual resistances are representing local voltage/current slopes which were integrated to obtain individual fuel electrode related overpotentials. In order to evaluate the fuel electrode related charge-transfer overpotential, the ASR of the high-frequency (>10^3 Hz) arcs were quantified and integrated from 0.25 A cm^{-2} to the operating current density. Likewise, to assess the mass-transfer overpotential, the low-frequency (ca. 3 Hz) arc was quantified and integrated in the same manner. The contribution of the diffusion resistance to the mass-transfer overpotential was in all cases minor and thus considered as negligible.

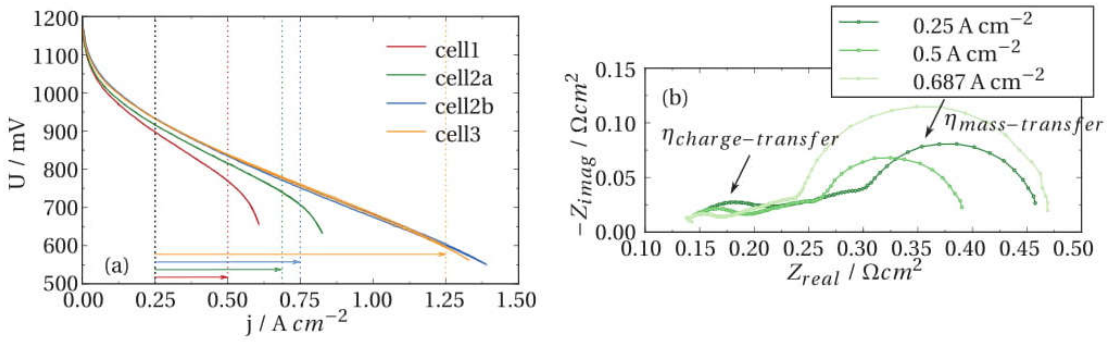

Figure 1 Quantification of charge- and mass-transfer overpotential via integration of local current/voltage slopes after overcoming activation losses (a) and corresponding EIS measurements of cell 2a at individual current density steps used for quantification of individual overpotential contributions (b).

Degradation rate

To evaluate the electrochemical DR_{ASR} the following standard conditions are chosen (equally to the standard conditions proposed in a previous study [6]): 750°C, 20:80 H_2O:H_2 fuel to the fuel electrode and air to the oxygen electrode at OCV and were calculated according to

$$DR_{i,ASR} = (ASR_{i,final} - ASR_{i,initial})/ASR_{i,initial} \quad (1)$$

where ASR_i corresponds to the area specific resistance of component *i* determined from EIS measurements at OCV standard conditions before and after durability testing.

Microstructural Investigations

Systematic post-test analysis was performed by means of 2D SEM image analysis on approx.1 cm long polished cell cross sections using a low acceleration voltage contrast imaging technique to distinguish between percolating and non-percolating nickel [23]. Microstructural studies of the individual cells were performed for in- and outlet segments with a size of 100 µm x 12-15 µm covering an area of the active layer varying from 8400 - 13300 μm^2 for each segment. Quantitative analysis of the area of percolating Ni was performed as described in Ref. [24]

Results and Discussion

Electrochemical test

Part A. All four cells were operated for 350 h in a fuel composition of H_2O:H_2 70:30, yet low FU to avoid developing of large longitudinal gradients of steam over the fuel electrode. This conditioning process was performed based on a previous study [13] and should increase the possibility to study long-term degradation effects of the Ni-YSZ fuel electrode. In this study it could be shown that a higher initial steam content in the fuel resulted in a faster stabilization of Ni-YSZ degradation. In part A of the test the fuel electrode DR_{ASR} varied from 31-41 % for the four cells in the 350 h, with no apparent dependency upon current density (0.5 vs. 1 A cm^{-2}). Furthermore, no obvious degradation of serial resistances was detected (between -2.3 and 3.8%) and a small degradation of the oxygen electrode (0 – 15 %) occurred. This observation underlines time-to-degradation distributions due to arbitrary effects even if apparently identical tests (i.e. two cells each were operated at the same conditions) are performed.

Part B. The operating conditions of part B were chosen to simulate realistic operating conditions, meaning 750°C, high FU and dry H_2 fuel gas balanced with N_2 which in some stack technologies is needed to allow sufficient gas flow through a stack. In the following the impact of overpotential on the degradation of cell 1, cell 2a and cell 3 (stepwise increasing both charge- and mass-transfer overpotential of fuel electrode) will be compared and likewise cell 2a and cell 2b (with initial equal charge-transfer overpotential of fuel electrode with deviating mass-transfer overpotential) will be discussed.

To evaluate the electrochemical DR_{ASR} over time, EIS measurements at OCV standard conditions were performed and quantitatively analyzed. In Figure 2 the corresponding Nyquist plots of the individual cells and the calculated DR are given. The resulting DR of cell 1, 2a and 3 clearly indicated an obvious effect upon charge-transfer and mass-transfer overpotential. Increasing the fuel electrode charge-transfer overpotential from 0.02 V to 0.03 V and to 0.06 V and concurrently increasing the mass-transfer overpotential from 0.06 V to 0.085V and to 0.115 V resulted in an increasing $DR_{ASR,fuelelectrode}$ from 25 to 43 and to 170%, respectively. Similarly, this trend could also be observed in the case of $DR_{ASR,serial}$ which increased from 5 to 9 and to 12 %.

Comparison of cell 2a and cell 2b with the initially same calculated charge-transfer overpotential (ca. 0.03V) but deviating mass-transfer overpotential (0.085 V vs. 0.05 V), revealed no clear effect upon fuel electrode degradation as the DR_{ASR} only deviated by 7% and thus was considered a statistical deviation.

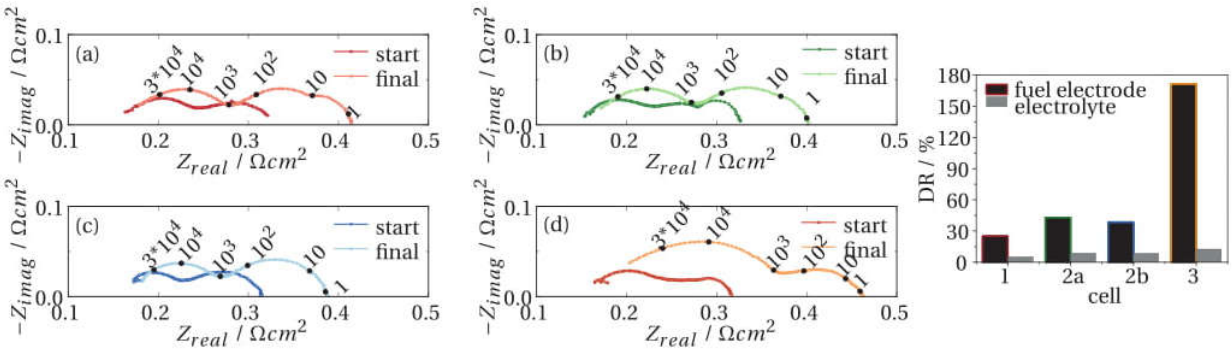

Figure 2 Time dependent Nyquist plots of cell 1(red) cell 2a (green) cell 3 (orange) cell 2b (blue) at standardized conditions, i.e. 750°C, 20:80 H_2O:H_2 fuel to the fuel electrode and air to the oxygen electrode at OCV, and corresponding DR on the right.

As the determined fuel electrode DRs from EIS only give averaged values over the whole electrode area, only locally performed *post-mortem* microstructural investigations allow a complementary view on the effect of overpotential.

Microstructural investigation

Qualitative studies of percolation – presented in Figure 3 – of cell 1-3 revealed clear deviations between in- and outlet segments.

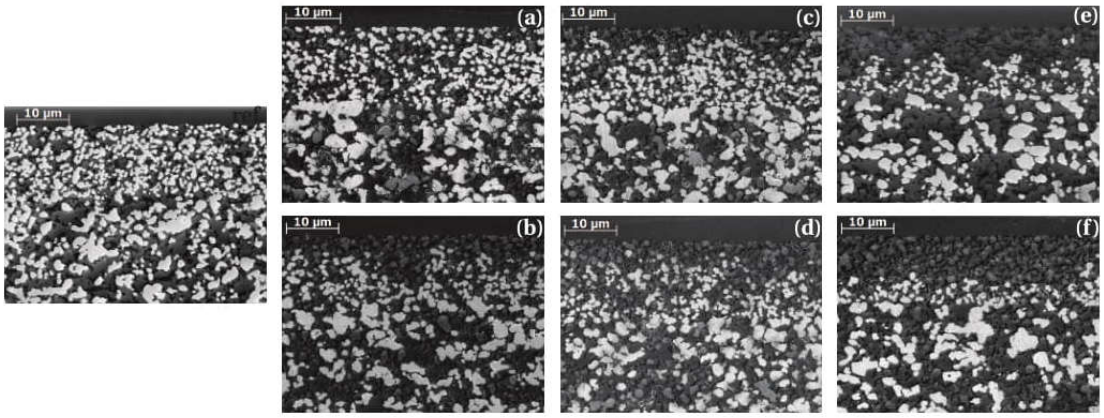

Figure 3 Qualitative percolation investigation of cell 1 inlet a) and outlet b), cell 2a inlet c) and outlet d) and cell 3 inlet e) and outlet f). The reference microstructure is given on the left. The electrolyte is at the top part of the images, followed by active Ni-YSZ electrode and Ni-YSZ support.

The quantitative analysis is shown in Figure 4. The different applied operating current densities (affecting both the charge-transfer and the mass-transfer overpotentials) are reflected in the microstructural results, by a decrease of the density of Ni-Ni contact points near the electrolyte. In case of cell 1-3, the phenomenon is more pronounced at the outlet than at the inlet. For cell 2b the effect of inlet and outlet are comparable (see Figure 4b). The decrease of Ni-Ni contact points, moreover results in a loss of Triple Phase Boundary (TPB) in the inner part of the electrode which shifted the active electrode/electrolyte interface into the fuel electrode, thereby effectively increasing the electrolyte thickness. The concomitant increase of the oxygen ion diffusion pathway is in good agreement with the increased serial resistance detected in the EIS study of the individual cells (R_s increased by 8, 13 and 20 mΩ cm^2 for cell 1 to 3). Overall, the observed degradation is in

good correlation with former studies on fuel electrode degradation [25,24] and thus the experiment did not cause any unforeseen 'degradation modes' which would not occur in real life operation.

The microstructural observation seemed therefore distinctly connected to the noticed electrochemical degradation pattern. The reduction of active TPB length (indicated in the loss of Ni-Ni connections) led to an increased $ASR_{fuelelectrode}$ whereas the increased electrolyte thickness can be seen from $DR_{ASR,serial}$. This in turn allowed basing the degradation prediction model on a material specific microstructural parameter, i.e. the percolation level of the Ni-network for anticipating fuel electrode degradation.

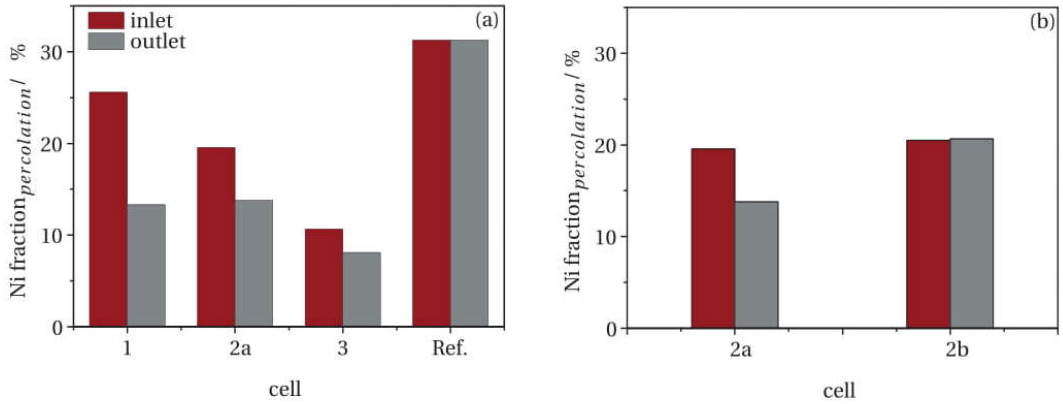

Figure 4 Quantitative comparison of the 2D percolation study. Nickel fraction of percolating Ni in the fuel electrode of cell 1, 2a and 3 (a), and cell 2a and 2b (b) at in- and outlet segment. The investigated area of the active layer for each segment was >8400 μm^2.

Degradation-stress dependency

In order to choose a semi-empirical prediction model for AT, it is essential to distinguish contribution from the different possible '*stress variables*'. The underlying phenomena are therefore addressed. As expected, cell operation with FU ≥ 70 % caused a significant longitudinal steam gradient across the cell. Thus, certainly FU can be accounted for as steam '*stress*' which is obviously the source of the deviations between in- and outlet segment. In the outlet segment, steam can be expected to highly contribute to the mass-transfer overpotential by changing severely the $p(H_2)/p(H_2O)$ ratio, on the contrary this contribution might be negligible for the inlet segment of the cell.

Furthermore, microstructural comparison of cell 2a and cell 2b, operated at similar initial charge-transfer overpotentials for the fuel electrode but different FU supports the influence of steam (see Figure 3b) as compared to an effect of the overpotential. Whereas the nickel phase percolation in cell 2a shows clear differences between the in- and outlet cell segments, this is not the case for cell 2b operated at lower FU, for which percolation level of the nickel phase within in- and outlet segments phase are similar. The amounts of percolating nickel are reduced by 38 to 34 % respect to the pristine Ni-YSZ structure, respectively.

Apart from the longitudinal steam gradient (stress steam), the degradation behavior due to different current density needs to be addressed. Apparently higher current density seemed to enhance the percolation loss (pronounced seen in the inlet segment percolation analysis of the cells 1, 2a and 3). However, thermofluid modeling studies of SOFC [26] for counter and co-flow geometry as well as studies on segmented cells [27] show that the activity of the cell is enhanced for the inlet segment of the cell and decreases towards the

outlet segment. Still, in all cases more active Ni-TPBs were found in the inlet segment where actually the reaction rate (reflecting the local current density) can be expected to be the highest. Thus the effect of current density is not dominating, but rather overruled by the effect of steam. Therefore, the effect of current density may be simply a consequence of the actual local steam generation at the active sites.

As a consequence, the chosen testing matrix had an indirect impact on the local fuel gas composition and the developing gradients. As steam seemed to be the dominating influence and thus in turn affecting charge and mass-transfer overpotential, an inverse power law relationship was considered to describe the impact on fuel electrode degradation [5].

Degradation prediction

For that reason, the charge-transfer overpotential as well as the mass-transfer overpotential was used as stress variable and the acceleration factor (AF) upon electrochemical fuel electrode degradation was described via a power-law relationship to extrapolate degradation under '*normal use*' conditions and stress conditions.

$$AF(s) = (\eta_s/\eta_0)^n \quad (2)$$

For quantification of the averaged fuel electrode degradation with respect to the electrochemical activity, two metrics determined from the SEM studies were considered. The inlet loss of percolation (Δin,ref) was taken as metric to evaluate the stress dependency upon different determined charge-transfer overpotential for the individual cells (where mass transport limitations of the reactive gases should be minimized) whereas the contribution expected due to variation of mass-transfer overpotential in the individual cells was assumed to be reflected in the declining deviation value between in- and outlet segment (Δin,out) *(*representative metric for the changes in developing fuel composition gradient due to the operating conditions).

The acceleration exponent n was determined via

$$n = [\partial \ln(\text{degradation metric}) / \partial \ln(\text{stress})]_{T,\,FU} \quad (3)$$

The results are shown in Figure 5. In both cases a power law dependency seems to be given. (R^2 =0.919 and R^2 =0.992)

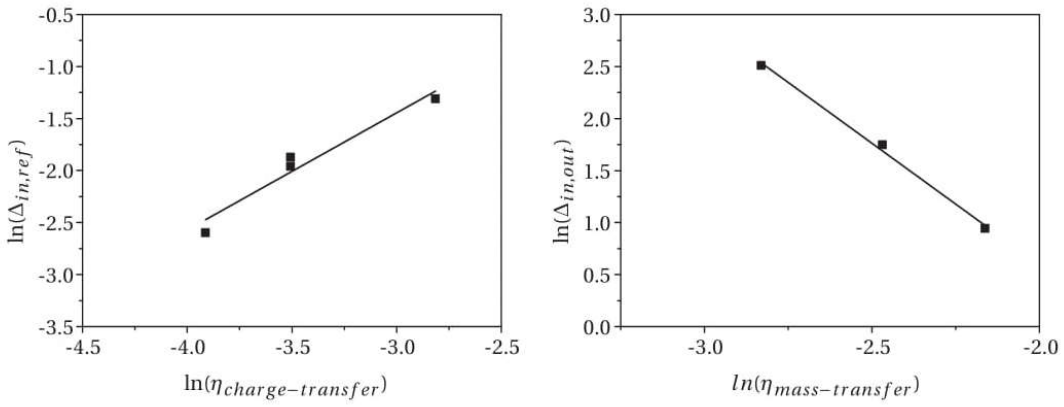

Figure 5 Dependency of Ni-YSZ degradation vs. stress conditions.

Via the acceleration exponent, the acceleration factor for each individual contribution was determined (see Figure 6), based on the assumption that cell 1 represents the normal

use operating conditions. In the investigated range, the impacts of both contributions seem to be similar. However in case of an increased mass-transfer limitation (e.g. higher FU = higher steam in the outlet segment) the impact of the mass-transfer overpotential will surpass the charge-transfer overpotential acceleration impact, indicated by the higher power-law exponent (2.4 vs. 1.1).

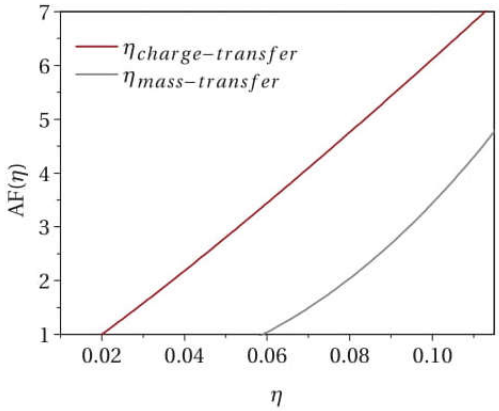

Figure 6 AF factor determined from material specific degradation for charge and mass-transfer limitations.

In the final step, the applicability of the degradation model based on the material specific parameter was evaluated. Taking both acceleration factors into account for cell 1, 2a and 3 and only the charge-transfer overpotential for cell 2b, the ASR increase was modeled and confronted with the experimental values determined from the EIS study. In Figure 7 the model predicted DR and the experimental result is shown. The model clearly captures the trend. Yet, in order to minimize the error range of ± 10% and to improve degradation prediction, more statistics are certainly favorable to account for arbitrary effects naturally occurring for experimentally based stress testing.

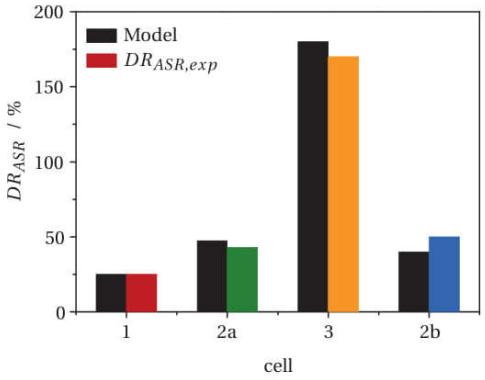

Figure 7 Correlation between AT model based on material specific property (i.e. percolation of Ni) with DR data experimental determined from standardized EIS measurements.

Conclusion

In this study an accelerated *calendar life* test approach for SOFC under realistic operating conditions was presented. Four fuel electrode supported SOFCs were tested at different overpotential stress conditions. A microstructural based degradation metric was proposed to quantify Ni-YSZ electrode aging. The degradation metric showed a clear power-law dependency upon stress conditions. The applicability of a semi-empirical based

prediction model on a material specific parameter was furthermore validated, by successfully predicting the corresponding electrochemical resistance increase.

Therefore, the established model is a valuable method for degradation comparison of different cell technologies as it does not rely on standardized testing conditions. Furthermore, with the presented method it seems to be possible to correlate DR based on microstructural properties with electrochemical based DRs.

References

[1] in *Solid Oxide Fuel Cell Lifetime and Reliability,* (Eds. N. Brandon, E. Ruiz-Trejo, B. Paul), Academic Press, **2017**.

[2] J. Schmalstieg, S. Käbitz, M. Ecker, D. U. Sauer, *J. Power Sources* **2014,** *257*, 325-334.

[3] J. W. McPherson in *Reliability Physics and Engineering: Time-to-failure modeling,* Springer International Publishing Schwitzerland, **2013**.

[4] M. S. Khan, S.-B. Lee, R.-H. Song, J.-W. Lee, T.-H. Lim, S.-J. Park, *Ceram. Int.* **2016,** *42*, 35-48.

[5] S. P. Jiang, X. Chen, *Int. J. Hydrogen Energy* **2014,** *39*, 505-531.

[6] A. Ploner, A. Hagen, A. Hauch, *Fuel Cells* **2017**.

[7] J. Sehested, J. A. P. Gelten, S. Helveg, *Appl. Catal., A* **2006,** *309*, 237-246.

[8] W. Nelson in *Accelerated Life Testing: Statistical Models, Test Plans and Data Analysis,* John Wiley & Sons New York, **2004**.

[9] L. A. Escobar, W. Q. Meeker, *Statist. Sci.* **2006,** *21*, 552-577.

[10] A. Hagen, R. Barfod, P. V. Hendriksen, Y.-L. Liu, S. Ramousse, *J. Electrochem. Soc.* **2006,** *153*, A1165-A1171.

[11] M. V. Ananyev, D. I. Bronin, D. A. Osinkin, V. A. Eremin, R. Steinberger-Wilckens, L. G. J. Haart, J. Mertens, *J. Power Sources* **2015,** *286*, 414-426.

[12] L. Holzer, B. Iwanschitz, T. Hocker, B. Münch, M. Prestat, D. Wiedenmann, U. Vogt, P. Holtappels, J. Sfeir, A. Mai, T. Graule, *J. Power Sources* **2011,** *196*, 1279-1294.

[13] A. Hauch, M. Mogensen, A. Hagen, *Solid State Ionics* **2011,** *192*, 547-551.

[14] M. J. Heneka, E. Ivers-Tiffée, *ECS Trans.* **2006,** *1*, 377-384.

[15] M. J. Heneka, E. Ivers-Tiffée, *J. Fuel Cell Sci. Technol.* **2011,** *9*, 11001-11001.

[16] A. Hagen, J. V. T. Høgh, R. Barfod, *J. Power Sources* **2015,** *300*, 223-228.

[17] A. Nakajo, P. Tanasini, S. Diethelm, J. Van herle, D. Favrat, *J. Electrochem. Soc.* **2011,** *158*, B1102-B1118.

[18] R. S. Gemmen, M. C. Williams, K. Gerdes, *J. Power Sources* **2008,** *184*, 251-259.

[19] A. Weber in *Encyclopedia of electrochemical power sources,* (Ed. J. Garche), Elsevier, Amsterdam, **2009**; 3 vols., pp 120-134, Fuel Cells - Solid Oxide Fuel Cells: Life Limiting Considerations.

[20] M. Jouin, M. Bressel, S. Morando, R. Gouriveau, D. Hissel, M.-C. Péra, N. Zerhouni, S. Jemei, M. Hilairet, B. Bouamama, *Appl. Energy* **2016,** *177*, 87-97.

[21] T. L. Skafte, J. Hjelm, P. Blennow, C. Graves, *Proceedings of 12th European SOFC & SOE Forum* **2016,** *Chapter 6*, 8-26.

[22] T. Ramos, J. Hjelm, M. Mogensen, *Journal of The Electrochemical Society* **2011,** *158*, B814-B824.

[23] K. Thydén, Y. L. Liu, J. B. Bilde-Sørensen, *Solid State Ionics* **2008,** *178*, 1984-1989.

[24] A. Hauch, P. S. Jørgensen, K. Brodersen, M. Mogensen, *J. Power Sources* **2011,** *196*, 8931-8941.

[25] S. D. Angelis, P. S. Jørgensen, E. H. R. Tsai, M. Holler, K. Kreka, J. R. Bowen,

Journal of Power Sources **2018,** *383*, 72-79.
[26] K. P. Recknagle, R. E. Williford, L. A. Chick, D. R. Rector, M. A. Khaleel, *J. Power Sources* **2003,** *113*, 109-114.
[27] W. G. Bessler, S. Gewies, C. Willich, G. Schiller, K. A. Friedrich, *Fuel Cells* **2010,** *10*, 411-418.

Acknowledgement

The authors would like to thank the colleagues at DLR Stuttgart - Patric Szabo and Aziz Nechache - for technical assistance in the laboratory. Furthermore, funding by the European project EU-INSIGHT (grant agreement No. 735918) is gratefully acknowledged.